

In this work, Tiszenkel et al. reported measurements of NH₃ and C1-C6 amines using an EtOH-CIMS equipped with a quadrupole mass filter (QMS) (Benson et al., 2010) at an urban site in Houston, TX. The ion chemistry and the methodology were well established. The calibration procedure and background checks were OK. However, only one major issue needs to be addressed before this manuscript can be accepted for publication. Previous work has shown that amides can also be detected by the EtOH-CIMS equipped with an HR-ToF-MS (Yao et al., 2016). It required at least a mass resolution of ~2500 to separate amines from amides. Amines are very photochemically active and can be oxidized swiftly into amides. It is reasonable to suspect significant amounts of amides were present in Houston, too. It is essential to assess the potential interferences from amides when measuring amines with a QMS-based EtOH-CIMS.

Response: Agreed. We have included a discussion of amide interference in the results and discussion section:

“It is possible that measured concentrations of amines measured here contain some interference from amides formed from oxidation of emitted amines. The CIMS does not have sufficient resolving power to separate trimethylamine (m/z 59.11) from acetamide (m/z 59.07), for example. Therefore, these amine concentrations represent an upper limit of amine concentrations (assuming all of the detected signal is due to the presence of amines). However, [Yao et al., 2016] measured amide concentrations in urban Shanghai in the tens to hundreds of pptv, while C1-C2 amine concentrations in Shanghai were similar to Houston observations reported here. Considering the consistency between amine measurements at these two urban locations, it is likely that interference from amides in the CIMS was minimal for C1 and C2 amines. The discrepancies between these two urban areas become more pronounced for C3-C6 amines (Table 1), which makes amide interference a possible explanation for elevated concentrations of C3 amines and above.”

The manuscript “Measurement Report : Urban Ammonia and Amines in Houston, Texas” reports observations of ammonia and c1-c6 amines in Houston, TX made with a quadrupole mass spectrometer utilizing a protonated ethanol detection scheme, i.e. EtOH Quad-CIMS technique. The observations were correlated with carbon dioxide which the authors interpret as indication of the ammonia and amines being emitted from pollution sources. As both ammonia and amines showed higher levels in the afternoon, the authors claim this indicates ‘dominant gas-to-particle conversion processes taking place with the changing ambient temperatures’. They also claim that from these observations globe models should use scaled down ammonia concentrations as a proxy for urban dimethylamine concentrations to simulate urban new particle formation processes in global models. These are significant claims not well supported by the data or analysis presented here. There is no particle information to substantiate that gas-to-particle conversion is occurring and the changes with ambient temperature are not due to emission changes, deposition changes, or inlet effects. Extrapolating the correlation between ammonia and dimethylamine from these measurements from one site at 5 m for 19 days in downtown Houston to be representative of the whole Houston urban area is unsupported, let alone further extrapolating to global models.

The EtOH Quad-CIMS technique is established in the literature, however, the details specific and relevant to this set of measurements are lacking. The limit of detection is given but not adequately defined. How is it estimated from a 1-minute integration time? Is it the standard deviation of the signal? Or 2 times the standard deviation?

Response: The caption of Table S1 has been updated to reflect that detail:

“The detection limits are estimated as three times the standard deviation of the background signal over one minute. In comparison, we also included those previously reported with the same instrument nearly 10 years earlier by [*You et al.*, 2014], estimated with the same time resolution.”

The sensitivity is determined from calibrations using permeation tubes. What is the uncertainty of the permeation rate? How is it determined? How are they diluted and what is the uncertainty in the dilution step or steps?

Response: The materials and methods section now contains a statement defining these uncertainties:

“The uncertainty in the CIMS included error in the permeation sources, which ranged from 2% to 5% depending on the compound. The permeation sources were diluted in two stages using flow controllers that each had uncertainties of 1.5%. Total error in the calibration of the Ethanol CIMS was 6.7%. Overall uncertainty in the CIMS was 30%, accounting for calibration error, variability of ion signals, and inlet losses.”

Why is the total estimated uncertainty not provided for any of the measurements reported here, including the carbon dioxide and nitrogen oxide measurements?

Response: The materials and methods section now explicitly states:

“The uncertainty in trace gas (CO and NO_x) measurements arises from instrumental uncertainty in the Thermo 48c CO analyzer and Thermo 42c-TL NO_x analyzer. Zero correction was performed on this instrument daily by switching to a flow of zero air. The typical uncertainty of each of these instruments was 5%.”

If the text reports a 1 minute 2 e-folding time as the time response, why does Fig. S2 report a 1 e-folding time of 28 seconds?

Response: To highlight the response time of the instrument, the text states that the e-folding time is under 1 minute for all measured ammonia and amines. In the case of ammonia, the e-folding time was 28 seconds, which is why that is the value reported in Figure S2.

It is, also, curious that in the introduction of previous measurements made, this manuscript does not cite Nowak et al. 2010 which presents airborne observations of ammonia over Houston and the effect of ammonia plumes on new particle formation, especially given that Nowak et al. 2010 uses the same EtOH Quad-CIMS technique. Even though Nowak et al. 2010 does not report amines it is highly relevant to the ammonia observations and the discussions presented here. Nowak, J. B., J. A. Neuman, R. Bahreini, C. A. Brock, A. M. Middlebrook, A. G. Wollny, J. S. Holloway, J. Peischl, T. B. Ryerson, and F. C. Fehsenfeld (2010), Airborne observations of ammonia and ammonium nitrate formation over Houston, Texas, *J. Geophys. Res.*, 115, D22304, doi:10.1029/2010JD014195

Response: We have added this reference to the introduction and discussion of sources of ammonia concentrations in Houston:

“Previous CIMS ammonia measurements from aircraft flights above Houston observed similar baseline concentrations of ammonia (0.2-3 ppbv) with brief spikes in concentration (up to 80 ppbv) associated with agricultural or industrial activity [*Nowak et al.*, 2010].”

The correlations between the various observed species and temperature are difficult to ascertain from Fig. 4. The text states (line 205) ‘Amines generally showed linear relationships with temperature, with C3 and C4 amines displaying the strongest relationships’, but the variability in the ammonia and amine observations make this difficult to see, even if one ignores the vertical bars. Though the authors present an empirical parametrization of ammonia as a function of temperature, it is not on the figure to be evaluated visually.

Response: Figure 4 has been updated with linear fits and R² values in order to assist with visual evaluation of the measurements.

The discussion from lines 211 to 219 is very difficult to follow. It starts by stating ‘elevated temperatures generally result in heightened emissions of ammonia and amines.’ and continues to state ‘The clear temperature dependence of ammonia and amines indicates dominant gas-to-particle conversion processes’. Emissions and gas-to-particle conversion are two very different processes. The manuscript does not make it clear how to differentiate between those two without particle data. It then goes on to state a previous study ‘showed an anticorrelation of these base

compounds between gas and aerosol phases'. However, there is no information on base compounds in the aerosol phase provided here. It seems that the authors are saying that since a previous study was able to show that elevated temperatures affect gas-to-particle conversion then elevated temperatures here show the same even though this manuscript does not have the supporting data the previous study had. This ambiguity in the argument does not support the claim in the abstract that the observations indicate dominant gas-to-particle conversion processes are taking place with changing ambient temperatures during the study.

Response: We have clarified the language in this passage to be less speculative about our observations and more clearly separate emissions and gas-to-particle conversion:

“The temperature dependence of ammonia and amines was previously observed in a rural forest in Alabama by [You et al., 2014], which attributed this partially to particle-to-gas conversion of ammonia and amine containing particles at elevated temperatures. The temperature dependence could also be due to higher emissions at higher temperatures. The temperature dependence of ammonia and amines has been observed at other urban, suburban and rural locations such as Kent, Ohio [You et al., 2014], Atlanta [Hanson et al., 2011], Delaware [Freshour et al., 2014], the Southern Great Plains [Freshour et al., 2014], and rural central Germany [Kürten et al., 2016].”

The manuscript claims that the observed ratio of dimethylamine to ammonia should be used to parameterize urban dimethylamine concentrations in global models to simulate urban new particle formation. This ratio comes from the fit of ammonia to C2-amines in Figure 7. What exactly is plotted in Figure 7?

Response: Figure 7 shows the correlation of ammonia and binned C1-C6 amines measured during our observation period. The correlation of the raw 1-minute data and the binned data are the same. In order to provide more comprehensive information, the 1-minute data is now shown in Figure 7 in addition to the binned data. Additionally the linear fits for this data and r^2 values are now included in Figure 7.

The manuscript says the measurements have a 1-minute time resolution, but Figure 7 is not plotting the 1-minute ammonia observations versus 1-minute amine observations. It appears that the ammonia is binned by the ammine mixing ratio and then the ammonia average for each bin plotted. Why is that and what is the rationale? Why are the 1-minute observations not plotted against each other?

Response: As stated previously, the 1-minute data is now shown in Figure 7 in addition to the binned data. The rationale for only showing the binned data was that the 1-minute data has a great deal of noise that made it difficult to discern the correlation between ammonia and amines visually.

There are no horizontal bars included on the amine observations. If the data has been binned, then the bin width should be shown. It is assumed, though not stated that the ratio comes from the slope of the fit. What fit is used and has there been any weighting applied, if so to which variables?

Response: The bin width is now shown for all figures with binned data. The fits were linear regression analyses without any weighting to the variables.

Furthermore, lines 81-83 state ‘However, isomers of amines were still not resolved in the detection; for example, the measured C2-amines still contained dimethylamine and ethylamine. Thus, a major disadvantage of a mass spectrometer (regardless of mass resolution) is the inability to resolve/identify isomers.’ Thus, it is reasonable to conclude that the C2-amines in Fig. 7 could include ethylamine meaning the recommended parametrization is at best urban dimethylamine/ethylamine as 0.1% of ammonia. Any recommendation to a modeling community needs to be clarified and stated clearly.

Response: We have added a clarifying statement:

“However, this recommendation comes with the caveat that measured C2 amines may include dimethylamine as well as ethylamine due to the inability of mass spectrometry to resolve isomers. Therefore, this correlation represents only the upper bound of dimethylamine concentrations.”

We have also added additional clarifying language to the conclusions section:

“However, as the CIMS is incapable of resolving isomers, this parameterization is only capable of representing the upper bounds of amines. Further work involving instrumentation capable of isomer resolution such as tandem MS/MS or chromatographic separation is needed to determine typical isomer ratios of amines for more accurate parameterizations.”

The manuscript reports observations of species not regularly measured. However, the analysis is weak and does not support the conclusions the manuscript attempts to make. Therefore, it should be rejected, and the analysis reconsidered and redone.

1 **Measurement Report: Urban Ammonia and Amines in Houston, Texas**

2
3 Lee Tiszenkel¹, James Flynn², Shan-Hu Lee^{1*}

4
5 ¹ Department of Atmospheric and Earth Sciences, University of Alabama at Huntsville;
6 Huntsville, Alabama, USA

7 ² Department of Earth and Atmospheric Sciences, University of Houston; Houston, Texas,
8 USA

9
10 Corresponding author (shanhu.lee@uah.edu)

11

12 **Abstract.** Ammonia and amines play critical roles in secondary aerosol formation, especially in
13 urban environments. However, fast measurements of ammonia and amines in the atmosphere are
14 very scarce. We measured ammonia and amines with a chemical ionization mass spectrometer
15 (CIMS) at the urban center in Houston, Texas, the fourth most populated urban site in the United
16 States, during October 2022. Ammonia concentrations were on average 4 parts per billion in
17 volume (ppbv), while the concentration of an individual amine ranged from several parts per
18 trillion in volume (pptv) to hundreds of pptv. These reduced nitrogen compounds were more
19 abundant during the weekdays than on weekends and correlated with measured CO concentrations,
20 implying they were mostly emitted from pollutant sources. Both ammonia and amines showed a
21 distinct diurnal cycle, with higher concentrations in the warmer afternoon, indicating dominant
22 gas-to-particle conversion processes taking place with the changing ambient temperatures. Studies
23 have shown that dimethylamine is critical for urban new particle formation (NPF), but currently,
24 there are no amine emission inventories in global climate models (as opposed to ammonia). Our
25 observations show that amines in general positively correlated with ammonia, indicating that it is
26 reasonable for global models to use scaled-down ammonia concentrations (e.g., 0.1 %) as a proxy
27 of urban dimethylamine concentrations to simulate urban NPF processes.

28 **1. Introduction**

29 Atmospheric ammonia and amines are ubiquitous in the atmosphere, and they have been found
30 in the gas phase, aerosol, clouds, and fog droplets [*Ge et al.*, 2011a; b]. Ammonia and amines are
31 emitted from various natural and anthropogenic sources, such as agricultural activity, animal
32 husbandry, vegetation, soil, waste processing, automobile traffic, power plants, and biomass
33 burning [*Ge et al.*, 2011a]. Ammonia and amines often share the same emission sources. In general,
34 ambient concentrations of ammonia are at the parts per billion in volume (ppbv) range, and amines
35 are approximately two to three orders of magnitude lower than ammonia concentrations. Ambient
36 concentrations of ammonia and amines vary rapidly due to emission, gas-to-particle conversion,
37 and wet deposition processes [*You et al.*, 2014; *Yu and Lee*, 2012].

38 Laboratory studies have shown that ammonia and amines play key roles in new particle
39 formation (NPF) as they can stabilize sulfuric acid clusters [*Almeida et al.*, 2013; *Glasoe et al.*,
40 2015; *Jen et al.*, 2016; *Lehtipalo et al.*, 2018; *M Xiao et al.*, 2021; *Yu et al.*, 2012]. In particular,
41 dimethylamine can have a profound effect on atmospheric processes even at the pptv level
42 [*Almeida et al.*, 2013; *Glasoe et al.*, 2015]. Field observations show that ammonia and amines are
43 associated with NPF events in Chinese megacities [*R. Cai et al.*, 2021; *Runlong Cai et al.*, 2023;
44 *Yan et al.*, 2021; *Yao et al.*, 2016], urban areas in the United States [*Jen et al.*, 2016; *Smith et al.*,
45 2010], European cities [*J. Brean et al.*, 2020], a high altitude site [*Bianchi et al.*, 2016], and the
46 Arctic and Antarctic [*Beck et al.*, 2021; *James Brean et al.*, 2021; *Jokinen et al.*; *Köllner et al.*,
47 2017]. However, global models cannot simulate urban NPF processes currently because of the lack
48 of amine emission inventories in models.

49 Ammonia and amines also contribute to secondary organic aerosol (SOA) formation by
50 condensation of oxidation products formed by reactions with ozone, OH, or NO₃ radicals and

51 produce light-absorbing particles [Mark E. Erupe et al., 2010; Malloy et al., 2009; C. J. Nielsen,
52 2016; Claus J. Nielsen et al., 2012; Qiu and Zhang, 2013; Silva et al., 2008]. As a result, reducing
53 ammonia emissions has been identified as a cost-effective way to mitigate ambient fine particle
54 concentrations [Gu et al., 2021].

55 Fast-response measurements of ammonia and amines at atmospheric concentrations are very
56 challenging [Lee, 2022], although such measurements are necessary because these reduced
57 nitrogen compounds have relatively short atmospheric lifetimes [Claus J. Nielsen et al., 2012].
58 Previously, [Schwab et al., 2007] made an intercomparison of six different ammonia detection
59 methods in the laboratory and found a large variance in the measured concentrations and vastly
60 different response times (over several hours) within different instruments. Difficulties in the
61 detection of base compounds also arise because these “sticky” compounds can rapidly adsorb and
62 desorb on/from the surfaces of sampling inlets to cause background signals that vary depending
63 on ambient concentrations, air humidity, and other atmospheric conditions. Thus frequent, in situ
64 measurements of instrument background signals using proper zero gases are required, especially
65 for field observations with rapidly changing ambient concentrations of base compounds.

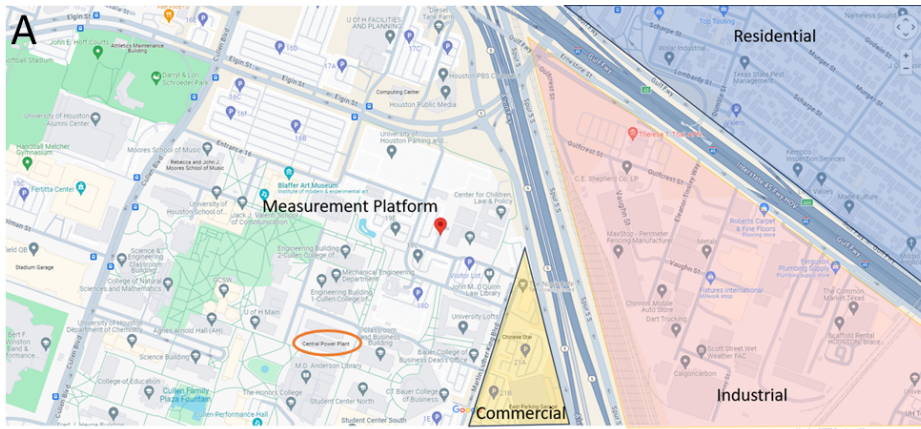
66 Chemical ionization mass spectrometers (CIMS) using ion reagents such as protonated ethanol,
67 acetone, and water ions can detect ammonia and amines in the atmosphere with fast response
68 [Benson et al., 2010; Hanson et al., 2011; Jen et al., 2016; Nowak et al., 2006; Nowak et al., 2010;
69 Yu and Lee, 2012]. As summarized in Table 1, CIMS technique has been used for the detection
70 of ambient ammonia and amines at a polluted site in Ohio [You et al., 2014; Yu and Lee, 2012], a
71 rural Alabama forest [You et al., 2014], and polluted urban sites in China [G Wang et al., 2016; M
72 Wang et al., 2020a; Zheng et al., 2015; Zhu et al., 2022]. As shown in Table 1, there are even
73 fewer studies that simultaneously measured ammonia and amines. The CIMS using ethanol reagent
74 can measure amines at or below single-digit pptv concentrations with a time response of 1 minute
75 and measure simultaneously amines and ammonia [Benson et al., 2010; M. E. Erupe et al., 2011;
76 You et al., 2014; Yu and Lee, 2012]. The CIMS using protonated water ions (i.e., proton-transfer
77 chemical ionization mass spectrometer, PTR-CIMS) can measure mono- and di-amines [Hanson
78 et al., 2011; Jen et al., 2016]. Using a high-resolution time-of-flight (HR-TOF) detector coupled
79 to CIMS (HR-TOF CIMS) (with ethanol reagent), [Yao et al., 2016] measured various amines and
80 amides in Shanghai. However, isomers of amines were still not resolved in the detection; for
81 example, the measured C2-amines still contained dimethylamine and ethylamine. Thus, a major
82 disadvantage of a mass spectrometer (regardless of mass resolution) is the inability to
83 resolve/identify isomers. To resolve isomers, tandem MS/MS analysis or an additional
84 independent separation method (such as chromatography) coupled to the mass spectrometer is
85 necessary.

86 In situ measurements of ammonia have been made in various atmospheric environments also
87 with optical techniques such as open-path absorption [Miller et al., 2014], closed-path absorption
88 [Ellis et al., 2010; Griffith and Galle, 2000; Leen et al., 2013; McManus et al., 2010; Pollack et
89 al., 2019], cavity ring-down spectroscopy [Martin et al., 2016], and photoacoustic spectroscopy

90 [Pushkarsky *et al.*, 2002]. These fast-response optical techniques were used for flux and aircraft
91 measurements of ammonia.

92 We measured ammonia and C1-C6 amines with an ethanol CIMS in October 2022 at the urban
93 center in Houston, Texas. Houston is the fourth most populated urban center in the U.S. and
94 contains a diverse range of pollutant emissions from urban activity, traffic, ship channels, oil
95 production, marine air masses, and agricultural activity. The primary goal of these measurements
96 is to quantify ammonia and C1-C6 amines in an urban setting and identify the atmospheric
97 conditions that affect their abundance. The study is amongst very few observations of ammonia
98 and amines at highly polluted urban sites in the U.S. We also compare observations in Houston
99 with previous measurements taken with the same instrument in Kent, Ohio (less polluted) [You *et al.*,
100 2014] and establish a quantitative relationship between ammonia and dimethylamine in a
101 different range of polluted conditions. This relationship will allow global models to simulate urban
102 NPF processes using the existing ammonia emission inventories.

103 2. Methods

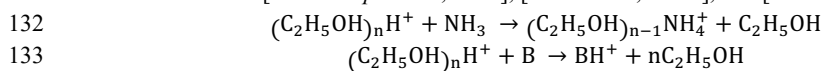


106
107
108 **Figure 1.** Location of the measurement platform, indicated by a red pin in the center of the map.
109 Nearby commercial, industrial, and residential areas are labeled by yellow, red, and blue shaded
110 sections, respectively. The nearby University of Houston power plant is circled in orange to the
111 southwest of the measurement platform. The map of the greater Houston urban area, as well as
112 the satellite view of the nearby vicinity of the measurement site, are shown in Figure S1.

113
114 The field observation took place in Houston continuously from the 8th to the 27th of October in
115 2022. Measurements were made at a stationary platform located on the campus of the University
116 of Houston (29.72° N, 95.34° W) ~2.5 km from central downtown Houston. Maps of the
117 measurement site (Figures 1 and S1). The measurement platform was located ~5 m from an active

118 parking lot, ~200 m from a low-traffic road, ~300 m from a high-traffic thoroughfare, and ~500 m
119 from an interstate highway. The immediate vicinity of the site was the University of Houston
120 campus, containing classroom buildings, dormitories, facilities services, and dining halls. Nearby
121 to the southeast of the site were several restaurants as well as an industrial park containing sites of
122 chemical supply companies, construction, machining services, and automobile shops. The site was
123 surrounded by residential areas to the south, northeast, and west. The city center and highest
124 population densities were to the northeast of the measurement site.

125
126 The ethanol CIMS instrument used has been described in detail previously [Benson *et al.*,
127 2010; You *et al.*, 2014; Yu and Lee, 2012]. The CIMS draws 10 standard liter per minute (slpm)
128 of sample air into a low-pressure ion-molecule region (about 2,000 Pa) where the flow mixes with
129 a pure nitrogen flow with a 2 slpm through a stainless-steel vessel of 200-proof ethanol, followed
130 by a ^{210}Po radiation source. Ammonia and amines were detected with the following ion-molecule
131 reactions based on [M. E. Erupe *et al.*, 2011], [Yu and Lee, 2012], and [Nowak *et al.*, 2006]:



134 Here, “B” refers to amines, and “n” is the number of reagent ions measured by the CIMS (n=1-3).
135 The $(\text{C}_2\text{H}_5\text{OH})_2\text{H}^+$ (m/z = 93) peak was the highest among the three reagent ions (m/z = 47, 93,
136 and 140). As shown in Figure S2, the production ions of amines were protonated ions: C1-amine
137 (m/z = 32), C2 (m/z = 46), C3 (m/z = 60), C4 (m/z = 74), C5 (m/z = 88), and C6 (m/z = 102).
138 Ammonia product ions were NH_4^+ (m/z = 18, higher peak) and $(\text{C}_2\text{H}_5\text{OH})\text{NH}_4^+$ (m/z = 64, lower
139 peak); these two ions were strongly correlated to each other during the ammonia calibration and
140 ambient measurements, indicating they represent ammonia signals.

141 To obtain a background signal, the CIMS is operated with 10 minutes of sampling followed
142 by 10 minutes of background measurements. Figure S2 shows the main reagent and base
143 compound product ions during the switching between ambient and background measurements.
144 Background measurements were taken by switching a 3-way valve to supply the inlet with a flow
145 of zero air through a silicon phosphate medium (Pan Tech, Texas) to scrub ammonia and amines.
146 The reagent signal was taken as the sum of three ethanol reagent ions. Reagent ion signals were
147 typically around 400 kHz with less than 10 % difference between ambient and background
148 measurement modes. Ammonia and amine concentrations were calculated by the difference
149 between the ambient and background signals normalized to 1,000,000 Hz of reagent ion signal
150 multiplied by a calibration factor. Calibration of the instrument was carried out with diluted
151 ammonia in nitrogen and permeation tubes of methylamine, dimethylamine, trimethylamine,
152 diethylamine, and diisopropylamine (Kin-tek, USA). Due to the difficulty of obtaining a
153 calibration standard, C5 amines were assumed to have the same sensitivity as C6 amines. The
154 calibration factors for each compound and detection limits were found to be similar to the results
155 from the calibration of the instrument by [You *et al.*, 2014] (Table S1), over a period of nearly 10
156 years, demonstrating an excellent reproducibility in the instrument performance. The time
157 response of the CIMS instrument to ammonia and amines is defined as where the signal stabilizes

158 at its “double e-folded” concentration of $1/e^2$ during the calibration. Average response times for
159 ammonia and amines were smaller than 1 minute. For each 10-minute cycle of background and
160 measurement, the first two minutes of each background/measurement cycle were excluded from
161 the data analysis to allow the instrument to reach a steady concentration.

162 The uncertainty in the CIMS included error in the permeation sources, which ranged from 2%
163 to 5% depending on the compound. The permeation sources were diluted in two stages using flow
164 controllers that each had uncertainties of 1.5%. Total error in the calibration of the CIMS was
165 6.7%. Overall uncertainty in the CIMS was 30%, accounting for calibration error, variability of
166 ion signals, and inlet losses.

167 Meteorological data was measured concurrently on the platform by a Vaisala HMP-45c for
168 temperature and relative humidity, and a RM Young 05305 wind speed and direction sensor.
169 Additionally, CO and NO_x (NO+NO₂) were measured with Thermo 48c and Thermo 42c-TL,
170 respectively. These measurements were provided by the University of Houston. The uncertainty
171 in trace gas (CO and NO_x) measurements arises from instrumental uncertainty in the Thermo 48c
172 CO analyzer and Thermo 42c-TL NO_x analyzer. Zero correction was performed on this instrument
173 daily by switching to a flow of zero air. The typical uncertainty of each of these instruments was
174 5%.

Deleted: Ethanol

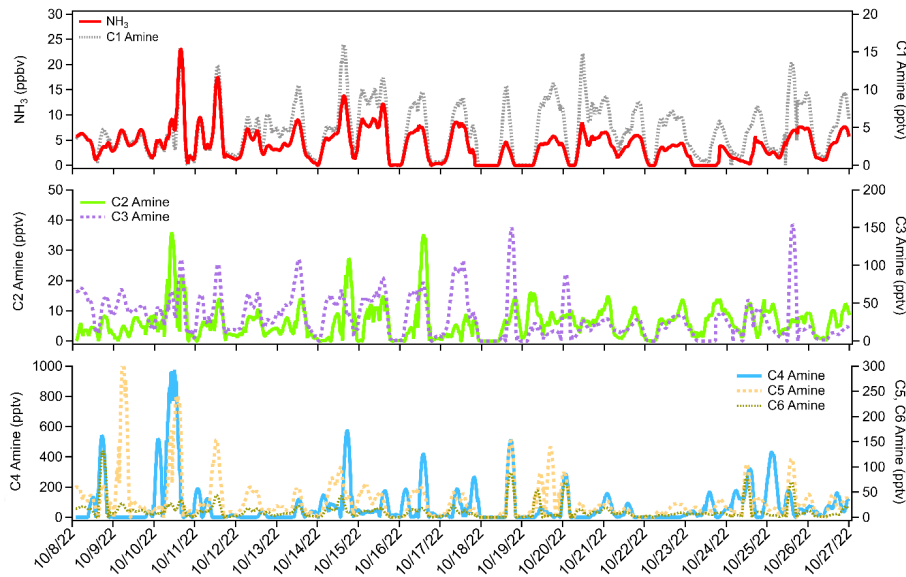
Formatted: Normal, Space After: 8 pt, Line spacing: Multiple 1.08 li

Deleted: Ethanol

Deleted: Ethanol

Formatted: Indent: First line: 0.25"

3. Results and Discussion



179

183 **Figure 2.** Time series of ammonia and C1-C6 amines observed at the urban center in Houston,
184 Texas, in October 2022.

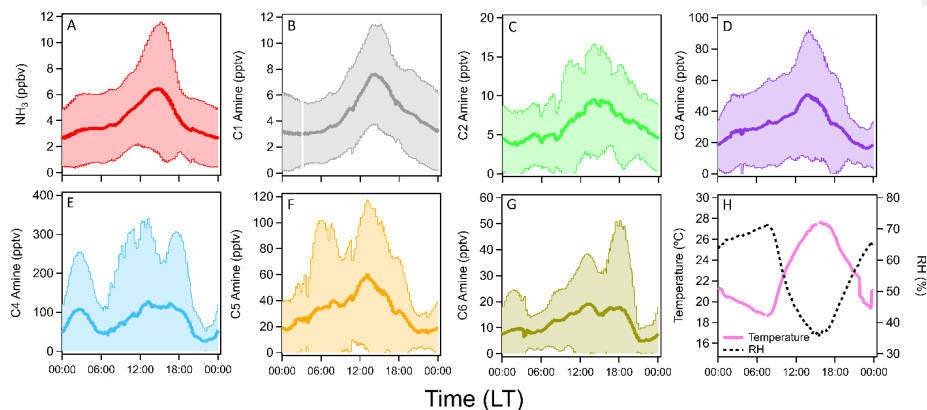
185 The time series of ammonia and amines during the ambient measurement period is shown in
186 Figure 2. The average ammonia concentration during the measurement campaign was 4 ppbv with
187 several short-term spikes above 10 ppbv and one occasion when the concentration exceeded 20
188 ppbv. Concentrations of C1 amine averaged 4 pptv with several spikes up to 15 pptv. Average C2
189 amine concentrations were 6 pptv with frequent but brief periods of concentrations more than 10
190 pptv. Average C3 amine concentrations were 31 pptv with brief increases in concentration above
191 100 pptv. C4 amine was the most abundant amine observed during the measurement period with
192 an average concentration of 79 pptv with spikes in concentration into the hundreds of pptv.
193 Average C5 and C6 amine concentrations were 33 and 12 pptv, respectively. These concentrations
194 in Houston were generally consistent with concentrations measured in other urban sites (Table 1).
195 Previous CIMS ammonia measurements from aircraft flights above Houston observed similar
196 baseline concentrations of ammonia (0.2-3 ppbv) with brief spikes in concentration (up to 80 ppbv)
197 associated with agricultural or industrial activity [Nowak et al., 2010]. Additionally, ammonia
198 concentrations of similar magnitude to the high spikes in concentration observed in this study have
199 been reported in Shanghai [S Xiao et al., 2015] as well as an urban site in Romania [Petrus et al.,
200 2022], with high ammonia concentrations corresponding to high temperatures and high traffic
201 activity. Long-term measurements taken in Nanjing with a cavity ring-down spectrometer also
202 showed an average ammonia concentration of 12 ppbv [Liu et al., 2024]. Measurements of amines
203 in Atlanta, Georgia showed <1 to 3 pptv concentrations of C1 and C2 amines, and C3 and C6
204 amines up to 15-25 pptv [Hanson et al., 2011]. Yao et al. [Yao et al., 2016] measured amines at
205 the level of pptv or sub-pptv, e.g., C2 amines of 3.9 ± 1.2 pptv, in urban Shanghai during the
206 summer. It is possible that measured concentrations of amines measured here contain some
207 interference from amides formed from oxidation of emitted amines. The CIMS does not have
208 sufficient resolving power to separate trimethylamine (m/z 59.11) from acetamide (m/z 59.07), for
209 example. Therefore, these amine concentrations represent an upper limit of amine concentrations
210 (assuming all of the detected signal is due to the presence of amines). However, [Yao et al., 2016]
211 measured amide concentrations in urban Shanghai in the tens to hundreds of pptv, while C1-C2
212 amine concentrations in Shanghai were similar to Houston observations reported here. Considering
213 the consistency between amine measurements at these two urban locations, it is likely that
214 interference from amides in the CIMS was minimal for C1 and C2 amines. The discrepancies
215 between these two urban areas become more pronounced for C3-C6 amines (Table 1), which
216 makes amide interference a possible explanation for elevated concentrations of C3 amines and
217 above.

Deleted: A

Deleted: Ethanol

Deleted: Ethanol

218



222

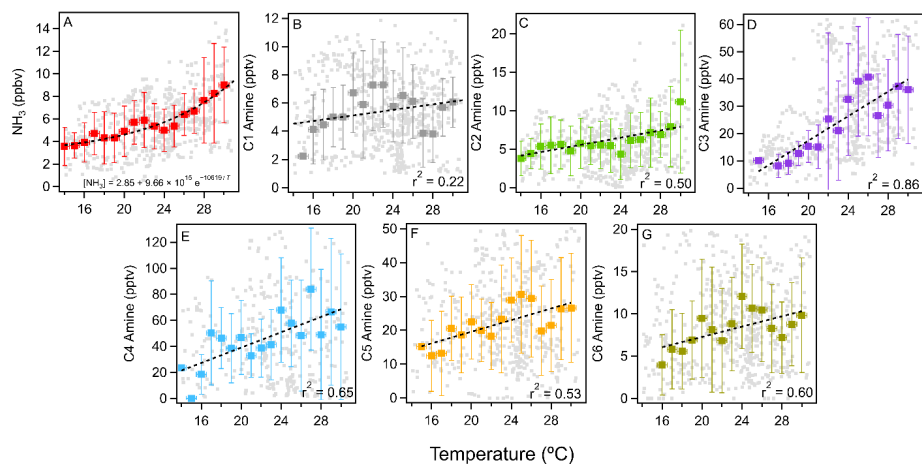
223 **Figure 3.** Averaged diurnal cycles of (a) ammonia, (b-g) C1-C6 amines, (h) temperature, and RH
 224 in Houston, Texas, during the observation period (19 days continuously). Shaded areas indicate 1
 225 standard deviation from the mean values of observation data.

226 Figure 3 shows the averaged diurnal concentrations of ammonia and amines during the
 227 observation period. Ammonia and amines had a diurnal cycle with peak concentrations in the
 228 afternoon with higher ambient temperatures. Generally, ammonia and amines correlated with one
 229 another throughout the measurement campaign, while C1-C3 amines showed the highest
 230 correlation with ammonia. Peak concentrations of all compounds corresponded with the high
 231 temperature of the day at around 3 pm local time. This was especially pronounced for ammonia,
 232 C1 and C3 amines. The relationships between ammonia and amines and temperature are shown in
 233 Figure 4. Ammonia had the strongest correlation with temperature, and the relationship fit an
 234 exponential parameterization, as the following:

235
$$[NH_3] = 2.85 + 9.66 \times 10^{15} e^{-\frac{10619}{T}}$$

236 Amines generally showed linear relationships with temperature, with C3 and C4 amines displaying
 237 the strongest relationships. C3 amines increased by 2.3 pptv per °C ($r^2 = 0.86$) and C4 by 2.9 pptv
 238 per °C ($r^2 = 0.65$). C5 and C6 amines were also moderately correlated with temperature, increasing
 239 by 1.2 pptv per °C and 0.5 pptv per °C, respectively ($r^2 = 0.60$ for both C5 and C6). On the other
 240 hand, the correlation of C1 and C2 amines with temperature were weaker: C1 only increased by
 241 0.1 pptv per °C with almost no correlation ($r^2 = 0.22$), and C2 increased by 0.8 pptv per °C ($r^2 =$
 242 0.50). The temperature dependence of ammonia and amines was previously observed in a rural
 243 forest in Alabama by [You *et al.*, 2014], which attributed this partially to particle-to-gas conversion
 244 of ammonia and amine containing particles at elevated temperatures. The temperature dependence
 245 could also be due to higher emissions at higher temperatures. The temperature dependence of
 246 ammonia and amines has been observed at other urban, suburban and rural locations such as Kent,

247 Ohio [You et al., 2014], Atlanta [Hanson et al., 2011], Delaware [Freshour et al., 2014], the
 248 Southern Great Plains [Freshour et al., 2014], and rural central Germany [Kürten et al., 2016].
 249

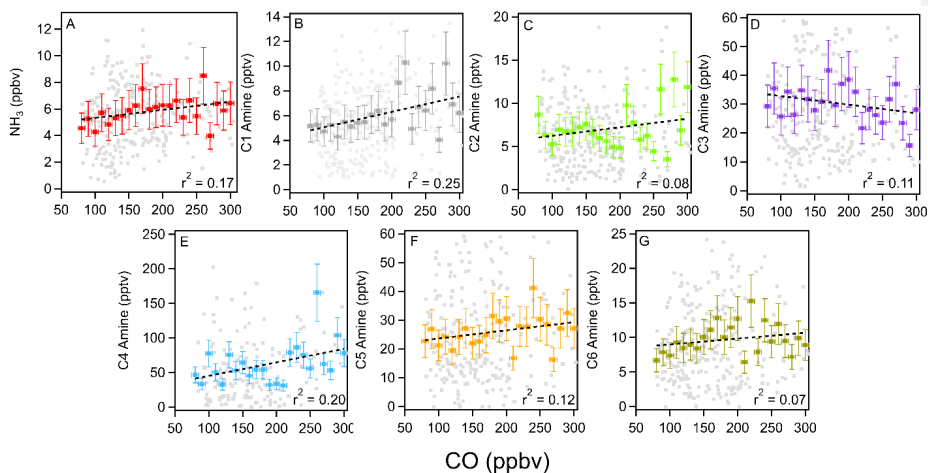


250
 251

252 **Figure 4.** Temperature dependence of (a) ammonia and (b-g) C1-C6 amines measured in Houston.
 253 Vertical bars indicate 1 standard deviation from the mean values of observation data. Binned
 254 temperatures are shown in colored squares. 1-minute averaged data is shown in gray squares.
 255 Horizontal bars indicate bin width. Black dashed lines indicate exponential fit for ammonia and
 256 linear fits for amines.

257 Anthropogenic pollutants such as CO and NO_x and CO can serve as tracers for industrial and
 258 traffic activities. Ammonia and amines in general showed a positive correlation with CO, with the
 259 exception of C3 amines (Figure 5). As ammonia, amines, and CO can be traced to traffic or
 260 industrial emissions, the positive relationship between these compounds implies that these base
 261 compounds were emitted from pollutant sources. Unlike with CO, there was a negative correlation
 262 with NO_x (Figure S3). This lack of a strong correlation between NO_x and ammonia was previously
 263 observed in Nanjing where a strong reduction in NO_x concentration during COVID-19 lockdown
 264 periods was not accompanied by an equivalent reduction in ammonia concentrations [Liu et al.,
 265 2024]. This may indicate some unique emission sources for ammonia and amines that do not co-
 266 emit NO_x.

267

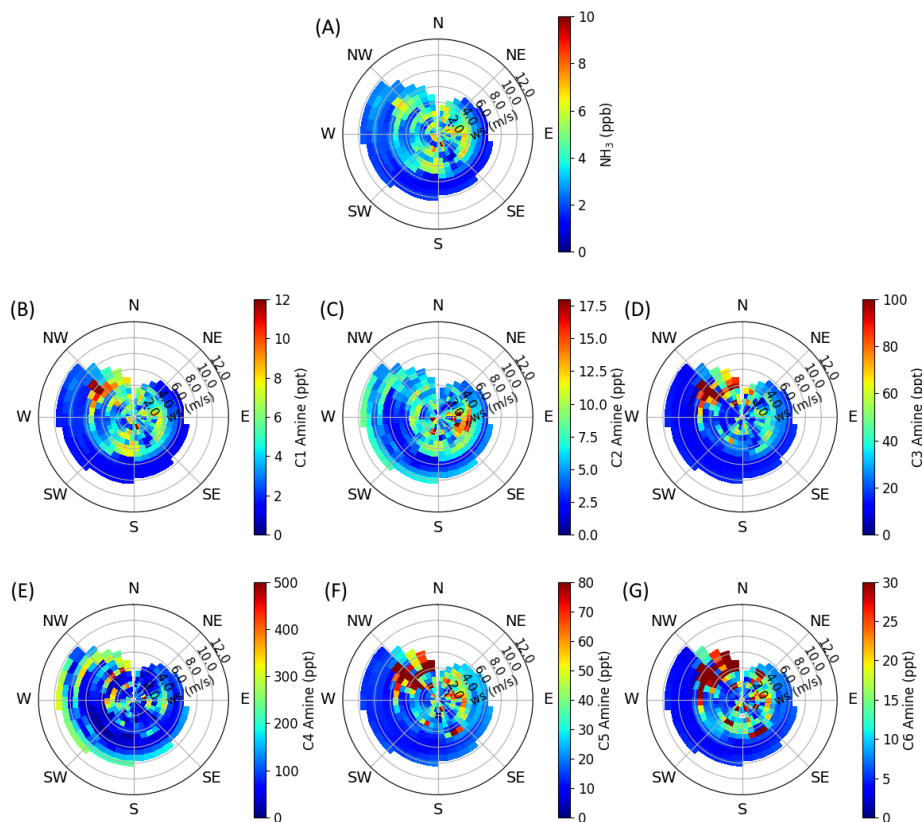


268
 269 **Figure 5.** Correlation between ammonia (a) and C1-C6 amines (b-g) with the collocated CO
 270 concentrations during the measurement campaign. Binned CO concentrations are shown in colored
 271 squares, 5-minute averaged data shown in gray squares. Vertical bars indicate 1 standard deviation
 272 from the mean values of observation data. Horizontal bars indicate bin widths. Black dashed lines
 273 indicate linear fits.

274 Wind speed and direction can help to identify local sources of ammonia and amines near the
 275 measurement site. Figures 6 and S4 show the correlation of ammonia and amines with wind speeds
 276 and direction throughout the observation period. Consistent between all base compounds is the
 277 high concentration coming from the southeast. This is the direction of the interstate highway,
 278 industrial areas, and train yards (Figures 1 and S1). Ammonia and most amines also have a
 279 pronounced source from the northwest – this is the direction of downtown Houston, where
 280 population density is highest. Except for C2 and C4 amines, the observed ammonia and amines in
 281 Houston were higher during periods of low wind speeds. The abundant C2 and C4 at high wind
 282 speeds may suggest that C2 and C4 amines were transported from more distant sources.

283 Figure S5 shows the average diurnal cycle of ammonia and amines on weekdays as opposed
 284 to weekends. Except for C2 and C4 amines, there was a clear decrease in concentrations during
 285 weekends during the afternoon peak. Weekends saw much less traffic and activity on the
 286 University of Houston campus. During this observation period, ambient temperatures were higher
 287 during the weekends, which would increase emissions. Therefore, the differences in weekdays vs.
 288 weekends indicate that amines and ammonia were indeed emitted from traffic and industrial
 289 activities. Lower average amine concentrations on weekends were also observed during mobile
 290 measurements in Yangtze River Delta cities [Chang *et al.*, 2022].

291
 292



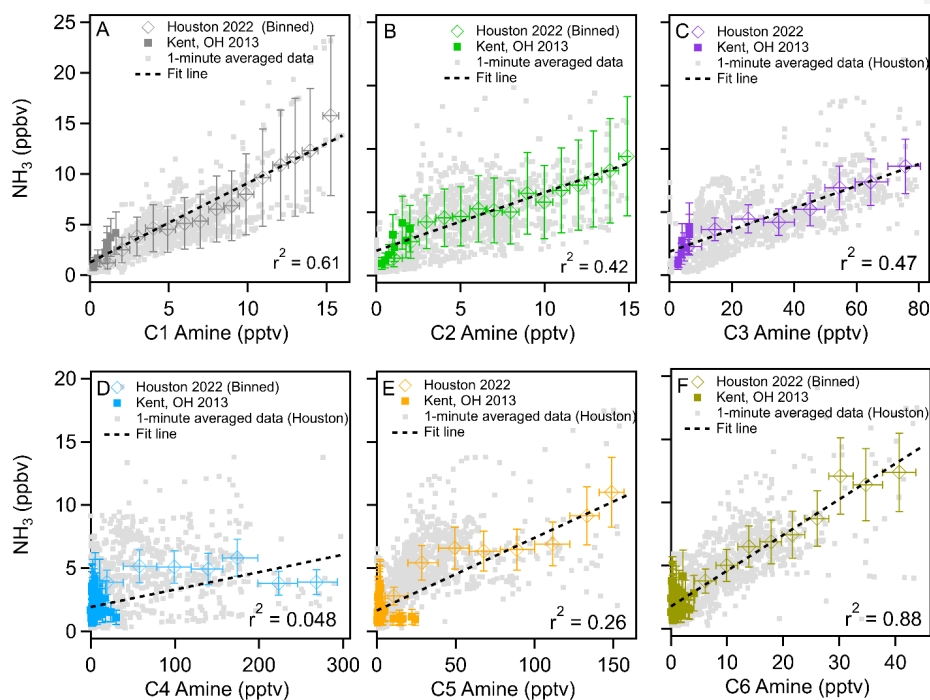
293
 294
 295 **Figure 6.** Wind rose plots of (a) ammonia and (b-g) C1-C6 amines observed in urban Houston.
 296 The color scale indicates concentration, and radial intensity shows wind speed.
 297

298 **4. Atmospheric Implications**
 299

300 Field observations show that sulfuric acid and amines are responsible for aerosol nucleation
 301 [J. Brean et al., 2020; R. Cai et al., 2021; Runlong Cai et al., 2023; Jen et al., 2016; Smith et al.,
 302 2010; Yan et al., 2021; Yao et al., 2016], however, currently, global models do not have amine
 303 emission inventories. Figure 7 shows the correlation of ammonia with C1-C6 amines measured
 304 during this campaign. This figure also includes that data obtained with the same instrument in
 305 Kent, Ohio, [You et al., 2014]. It is clear from this figure that concentrations of ammonia, C1, C2,
 306 C3, C5, and C6 amines were positively correlated with one another throughout the study: r^2 values
 307 for the correlation between ammonia and amines were 0.61 for C1, 0.42 for C2, 0.47 for C3, 0.26

308 for C5 and 0.88 for C6. These relationships imply that these compounds are mostly co-emitted
 309 from similar sources and undergo similar atmospheric transport. C4 amines showed no correlation
 310 with ammonia and lower-mass amines – the r^2 value for C4 vs. NH_3 was 0.048. This indicates a
 311 unique source for C4 amines, consistent with both elevated C4 concentrations at high wind speeds
 312 and higher weekend C4 concentrations as discussed previously. Correlations of C1-C3 amines
 313 concentrations, taken from the linear fits of the plots shown in Figure 7, were approximately
 314 equivalent to 1.1×10^{-3} [NH_3], 1.4×10^{-3} [NH_3], and 8.4×10^{-3} [NH_3], respectively. C5 and C6
 315 amine concentrations were 1.9×10^{-2} [NH_3] and 3.5×10^{-3} [NH_3], respectively (Table S2). From
 316 these results, we propose that global modelers use 0.1 % of the ammonia concentration as a proxy
 317 of dimethylamine to simulate urban NPF processes. However, this recommendation comes with
 318 the caveat that measured C2 amines may include dimethylamine as well as ethylamine due to the
 319 inability of mass spectrometry to resolve isomers. Therefore, this correlation represents only the
 320 upper bound of dimethylamine concentrations.

Deleted: Concentrations



322
 323 **Figure 7.** Correlations of C1-C6 amines with ammonia throughout the observation period in
 324 Houston (diamonds) and Kent, OH (squares) as reported by [You et al., 2014]. Binned
 325 concentrations are shown in colored squares. 1-minute averaged data from Houston are shown in

327 gray squares. Vertical bars indicate one standard deviation from the mean values of observation
328 data. Horizontal bars indicate bin widths. Black dashed lines indicate linear fits of the combined
329 data from Kent and Houston.

330 5. Conclusions

331 Our observations in urban Houston show that ammonia and amines generally followed a clear
332 diurnal cycle, peaking in the early afternoon when the ambient temperature was highest during the
333 day. We found a correlation of ammonia and amines with ambient temperature. The pronounced
334 diurnal cycles and temperature dependence of these compounds may be due to active partitioning
335 between the gas and particle phases, which is sensitively dependent on temperature. This could be
336 due to increased emissions of ammonia and amines from biogenic and anthropogenic sources. It
337 is likely a combination of these effects that causes elevated ammonia and amine concentrations
338 when temperatures are high.

339 High concentrations of ammonia and amines were correlated with local air masses from
340 densely populated areas and areas of high traffic, industry, and other human activity. This suggests
341 that most ammonia and amines measured in Houston originated from pollutant sources, consistent
342 with the correlation observed with CO concentrations. There was also a clear increase in ammonia
343 and amines on days with more human activity as shown by the results of concentrations on
344 weekends vs weekdays. We observed a consistent relationship between ammonia and amines
345 during our measurement campaign as well as with observations in less densely populated Kent,
346 Ohio, suggesting that it is reasonable to parameterize amine emission inventories based on existing
347 ammonia inventories to simulate urban NPF processes. However, as the CIMS is incapable of
348 resolving amides or isomers, this parameterization is only capable of representing the upper
349 bounds of amines. Further work involving instrumentation capable of isomer resolution such as
350 tandem MS/MS or chromatographic separation is needed to determine typical isomer ratios of
351 amines for more accurate parameterizations.

352 The CIMS used in this campaign is currently one of the few instruments in the world that is
353 capable of simultaneous measurements of ammonia and amines at atmospherically relevant
354 detection limits and timescales. Studies have shown that the co-presence of ammonia and amines
355 can enhance sulfuric acid nucleation rates compared to ammonia alone [*Glasoe et al.*, 2015; *Myllys*
356 *et al.*, 2019; *Yu et al.*, 2012]. From this perspective, simultaneous measurements of ammonia and
357 amines will be required for the correct prediction of NPF processes in the atmosphere.
358 Measurements of ammonia and amines with comprehensive calibration as shown in the present
359 study are very even rarer, but such measurements are needed for mitigating urban air quality
360 problems and the health effects of ultrafine particles.

362 Author Contributions

363 SHL designed the research; LT and SHL performed measurements; JF provided the measurement
364 platform as well as the trace gas and meteorology data; LT and SHL wrote the manuscript.

365 Acknowledgements

Deleted: Ethanol

367 We acknowledge funding support from National Science Foundation (grant numbers 2209722,
368 2117389, and 2107916) and Texas Commission on Environmental Quality (grant number 582-22-
369 31535-018).

370 **Table 1.** Ammonia and amine measurements with CIMS at various locations reported in the
 371 literature. DL, detection limit of each instrument.

Location	NH ₃ (ppbv)	C1 Amine (pptv)	C2 Amine (pptv)	C3 Amine (pptv)	C4 Amine (pptv)	C5 Amine (pptv)	C6 Amine (pptv)
Rural Alabama Forest [<i>You et al.</i> , 2014]*	Up to 1-2	< DL	< DL	1 - 10	< DL	< DL	< DL
Kent, Ohio [<i>You et al.</i> , 2014]*	Up to 6	1 – 4	< DL	5 - 10	10 - 50	10 - 100	< DL
Kent, Ohio [<i>Yu and Lee</i> , 2012]*	0.5 ± 0.26	-	8 ± 3	16 ± 7	-	-	-
Atlanta, Georgia [<i>Hanson et al.</i> , 2011]†	-	< 1	3	4 – 15	25	-	-
Lewes, Delaware [<i>Freshour et al.</i> , 2014]†	0.8	5	28	6	150	1	2
Lamont, Oklahoma [<i>Freshour et al.</i> , 2014]†	0.9	4	14	35	150	98	20
Minneapolis, Minnesota [<i>Freshour et al.</i> , 2014]†	1.8	4	42	19	14	20	5
Shanghai [<i>Yao et al.</i> , 2016]‡	-	3.9 ± 1.2	6.6 ± 1.2	0.4 ± 0.1	3.6 ± 1.0	0.7 ± 0.3	1.8 ± 0.8
Nanjing [<i>Zheng et al.</i> , 2015]‡	1.7 ± 2.3	7.2 ± 7.4 (C1 + C2 + C3)			-	-	-
Wangdu	-	-	14.6 ± 14.9	-	-	-	-

[Y Wang et al., 2020b]§							
Beijing [Zhu et al., 2022]‡	2.8 ± 2.0	5.2 ± 4.3 (C1 + C2 + C3)	-	-	-		
Houston, TX (This study)*	4 ± 1	4 ± 2	6 ± 2	31 ± 9	79 ± 30	33 ± 12	12 ± 4

372
373 * CIMS with ethanol reagent
374 † Proton-transfer chemical ionization mass spectrometer (PTR-CIMS)
375 ‡ High-resolution time of flight chemical ionization mass spectrometer (HR-TOF CIMS) with
376 ethanol reagent
377 § Vocus proton transfer time-of-flight mass spectrometer (PTR-TOF MS)
378
379

380 **References**

- 381
- 382 Almeida, J., et al. (2013), Molecular understanding of sulphuric acid–amine particle nucleation
383 in the atmosphere, *Nature*, 502(7471), 359-363, doi:10.1038/nature12663.
- 384 Beck, L. J., et al. (2021), Differing Mechanisms of New Particle Formation at Two Arctic Sites,
385 *Geophysical Research Letters*, 48(4), e2020GL091334,
386 doi:<https://doi.org/10.1029/2020GL091334>.
- 387 Benson, D. R., A. Markovich, M. Al-Refai, and S. H. Lee (2010), A Chemical Ionization Mass
388 Spectrometer for ambient measurements of Ammonia, *Atmos. Meas. Tech.*, 3(4), 1075-1087,
389 doi:10.5194/amt-3-1075-2010.
- 390 Bianchi, F., et al. (2016), New particle formation in the free troposphere: A question of
391 chemistry and timing, *Science*, 352(6289), 1109-1112, doi:10.1126/science.aad5456.
- 392 Brean, J., D. C. S. Beddows, Z. Shi, B. Temime-Roussel, N. Marchand, X. Querol, A. Alastuey,
393 M. C. Minguillón, and R. M. Harrison (2020), Molecular insights into new particle formation in
394 Barcelona, Spain, *Atmos. Chem. Phys.*, 20(16), 10029-10045, doi:10.5194/acp-20-10029-2020.
- 395 Brean, J., M. Dall’Osto, R. Simó, Z. Shi, D. C. S. Beddows, and R. M. Harrison (2021), Open
396 ocean and coastal new particle formation from sulfuric acid and amines around the Antarctic
397 Peninsula, *Nature Geoscience*, 14(6), 383-388, doi:10.1038/s41561-021-00751-y.
- 398 Cai, R., et al. (2021), Sulfuric acid–amine nucleation in urban Beijing, *Atmos. Chem. Phys.*,
399 21(4), 2457-2468, doi:10.5194/acp-21-2457-2021.
- 400 Cai, R., et al. (2023), Significant contributions of trimethylamine to sulfuric acid nucleation in
401 polluted environments, *npj Climate and Atmospheric Science*, 6(1), 75, doi:10.1038/s41612-023-
402 00405-3.
- 403 Chang, Y., et al. (2022), Nonagricultural Emissions Dominate Urban Atmospheric Amines as
404 Revealed by Mobile Measurements, *Geophysical Research Letters*, 49(10), e2021GL097640,
405 doi:<https://doi.org/10.1029/2021GL097640>.
- 406 Ellis, R. A., J. G. Murphy, E. Pattey, R. van Haarlem, J. M. O'Brien, and S. C. Herndon (2010),
407 Characterizing a Quantum Cascade Tunable Infrared Laser Differential Absorption Spectrometer
408 (QC-TILDAS) for measurements of atmospheric ammonia, *Atmos. Meas. Tech.*, 3(2), 397-406,
409 doi:10.5194/amt-3-397-2010.
- 410 Erupe, M. E., et al. (2010), Correlation of aerosol nucleation rate with sulfuric acid and ammonia
411 in Kent, Ohio: An atmospheric observation, *Journal of Geophysical Research: Atmospheres*,
412 115(D23), doi:<https://doi.org/10.1029/2010JD013942>.
- 413 Erupe, M. E., A. A. Viggiano, and S. H. Lee (2011), The effect of trimethylamine on
414 atmospheric nucleation involving H₂SO₄, *Atmos. Chem. Phys.*, 11, 4767-4775.
- 415 Freshour, N. A., K. K. Carlson, Y. A. Melka, S. Hinz, B. Panta, and D. R. Hanson (2014), Amine
416 permeation sources characterized with acid neutralization and sensitivities of an amine mass
417 spectrometer, *Atmos. Meas. Tech.*, 7(10), 3611-3621, doi:10.5194/amt-7-3611-2014.
- 418 Ge, X., A. S. Wexler, and S. L. Clegg (2011a), Atmospheric amines – Part I. A review,
419 *Atmospheric Environment*, 45(3), 524-546, doi:<https://doi.org/10.1016/j.atmosenv.2010.10.012>.
- 420 Ge, X., A. S. Wexler, and S. L. Clegg (2011b), Atmospheric amines – Part II. Thermodynamic
421 properties and gas/particle partitioning, *Atmospheric Environment*, 45(3), 561-577,
422 doi:<https://doi.org/10.1016/j.atmosenv.2010.10.013>.
- 423 Glasoe, W. A., K. Volz, B. Panta, N. Freshour, R. Bachman, D. R. Hanson, P. H. McMurry, and
424 C. Jen (2015), Sulfuric acid nucleation: an experimental study of the effect of seven bases, *J.*
425 *Geophys. Res.*, 120, 1933-1950, doi:Doi: 10.1002/2014JD022730.

426 Griffith, D. W. T., and B. Galle (2000), Flux measurements of NH₃, N₂O and CO₂ using dual
427 beam FTIR spectroscopy and the flux–gradient technique, *Atmospheric Environment*, 34(7),
428 1087-1098, doi:[https://doi.org/10.1016/S1352-2310\(99\)00368-4](https://doi.org/10.1016/S1352-2310(99)00368-4).
429 Gu, B., et al. (2021), Abating ammonia is more cost-effective than nitrogen oxides for mitigating
430 PM_{2.5} air pollution, *Science*, 374(6568), 758-762, doi:10.1126/science.abf8623.
431 Hanson, D. R., P. H. McMurry, J. Jiang, D. Tanner, and L. G. Huey (2011), Ambient Pressure
432 Proton Transfer Mass Spectrometry: Detection of Amines and Ammonia, *Environmental Science
433 & Technology*, 45(20), 8881-8888, doi:10.1021/es201819a.
434 Jen, C. N., R. Bachman, J. Zhao, P. H. McMurry, and D. R. Hanson (2016), Diamine-sulfuric
435 acid reactions are a potent source of new particle formation, *Geophysical Research Letters*,
436 43(2), 867-873, doi:<https://doi.org/10.1002/2015GL066958>.
437 Jokinen, T., et al. Ion-induced sulfuric acid–ammonia nucleation drives particle formation in
438 coastal Antarctica, *Science Advances*, 4(11), eaat9744, doi:10.1126/sciadv.aat9744.
439 Köllner, F., et al. (2017), Particulate trimethylamine in the summertime Canadian high Arctic
440 lower troposphere, *Atmos. Chem. Phys.*, 17(22), 13747-13766, doi:10.5194/acp-17-13747-2017.
441 Kürten, A., A. Bergen, M. Heinritzi, M. Leiminger, V. Lorenz, F. Piel, M. Simon, R. Sitals, A.
442 C. Wagner, and J. Curtius (2016), Observation of new particle formation and measurement of
443 sulfuric acid, ammonia, amines and highly oxidized organic molecules at a rural site in central
444 Germany, *Atmos. Chem. Phys.*, 16(19), 12793-12813, doi:10.5194/acp-16-12793-2016.
445 Lee, S.-H. (2022), Perspective on the Recent Measurements of Reduced Nitrogen Compounds in
446 the Atmosphere, *Frontiers in Environmental Science*, 10, doi:10.3389/fenvs.2022.868534.
447 Leen, J. B., X.-Y. Yu, M. Gupta, D. S. Baer, J. M. Hubbe, C. D. Kluzek, J. M. Tomlinson, and
448 M. R. Hubbell, II (2013), Fast In Situ Airborne Measurement of Ammonia Using a Mid-Infrared
449 Off-Axis ICOS Spectrometer, *Environmental Science & Technology*, 47(18), 10446-10453,
450 doi:10.1021/es401134u.
451 Lehtipalo, K., et al. (2018), Multicomponent new particle formation from sulfuric acid,
452 ammonia, and biogenic vapors, *Science Advances*, 4(12), eaau5363, doi:10.1126/sciadv.aau5363.
453 Liu, R., et al. (2024), Characteristics and sources of atmospheric ammonia at the SORPES
454 station in the western Yangtze river delta of China, *Atmospheric Environment*, 318, 120234,
455 doi:<https://doi.org/10.1016/j.atmosenv.2023.120234>.
456 Malloy, Q. G. J., Q. Li, B. Warren, D. R. Cocker III, M. E. Erupe, and P. J. Silva (2009),
457 Secondary organic aerosol formation from primary aliphatic amines with NO₃
458 radical, *Atmos. Chem. Phys.*, 9(6), 2051-2060, doi:10.5194/acp-9-2051-2009.
459 Martin, N. A., V. Ferracci, N. Cassidy, and J. A. Hoffnagle (2016), The application of a cavity
460 ring-down spectrometer to measurements of ambient ammonia using traceable primary standard
461 gas mixtures, *Applied Physics B*, 122(8), 219, doi:10.1007/s00340-016-6486-9.
462 McManus, J. B., S. Z. Mark, D. N. David, Jr., H. S. Joanne, C. H. Scott, C. W. Ezra, and W.
463 Rick (2010), Application of quantum cascade lasers to high-precision atmospheric trace gas
464 measurements, *Optical Engineering*, 49(11), 111124, doi:10.1117/1.3498782.
465 Miller, D. J., K. Sun, L. Tao, M. A. Khan, and M. A. Zondlo (2014), Open-path, quantum
466 cascade-laser-based sensor for high-resolution atmospheric ammonia measurements, *Atmos.
467 Meas. Tech.*, 7(1), 81-93, doi:10.5194/amt-7-81-2014.
468 Myllys, N., S. Chee, T. Olenius, M. Lawler, and J. Smith (2019), Molecular-Level
469 Understanding of Synergistic Effects in Sulfuric Acid–Amine–Ammonia Mixed Clusters, *The
470 Journal of Physical Chemistry A*, 123(12), 2420-2425, doi:10.1021/acs.jpca.9b00909.

471 Nielsen, C. J. (2016), Atmospheric Degradation of Amines (ADA). Summary report: Photo-
472 oxidation of methylamine, dimethylamine and trimethylamine. CLIMIT project no. 201604.,
473 *Norge: Norsk Institutt for Luftforskning*.

474 Nielsen, C. J., H. Herrmann, and C. Weller (2012), Atmospheric chemistry and environmental
475 impact of the use of amines in carbon capture and storage (CCS), *Chemical Society Reviews*,
476 *41*(19), 6684-6704, doi:10.1039/C2CS35059A.

477 Nowak, J. B., et al. (2006), Analysis of urban gas phase ammonia measurements from the 2002
478 Atlanta Aerosol Nucleation and Real-Time Characterization Experiment (ANARChE), *Journal*
479 *of Geophysical Research: Atmospheres*, *111*(D17), doi:<https://doi.org/10.1029/2006JD007113>.

480 Nowak, J. B., J. A. Neuman, R. Bahreini, C. A. Brock, A. M. Middlebrook, A. G. Wollny, J. S.
481 Holloway, J. Peischl, T. B. Ryerson, and F. C. Fehsenfeld (2010), Airborne observations of
482 ammonia and ammonium nitrate formation over Houston, Texas, *Journal of Geophysical*
483 *Research: Atmospheres*, *115*(D22), doi:<https://doi.org/10.1029/2010JD014195>.

484 Petrus, M., C. Popa, and A. M. Bratu (2022), Ammonia Concentration in Ambient Air in a Peri-
485 Urban Area Using a Laser Photoacoustic Spectroscopy Detector, *Materials (Basel)*, *15*(9),
486 doi:10.3390/ma15093182.

487 Pollack, I. B., J. Lindaas, J. R. Roscioli, M. Agnese, W. Permar, L. Hu, and E. V. Fischer (2019),
488 Evaluation of ambient ammonia measurements from a research aircraft using a closed-path QC-
489 TILDAS operated with active continuous passivation, *Atmos. Meas. Tech.*, *12*(7), 3717-3742,
490 doi:10.5194/amt-12-3717-2019.

491 Pushkarsky, M. B., M. E. Webber, O. Baghdassarian, L. R. Narasimhan, and C. K. N. Patel
492 (2002), Laser-based photoacoustic ammonia sensors for industrial applications, *Applied Physics*
493 *B*, *75*(2), 391-396, doi:10.1007/s00340-002-0967-8.

494 Qiu, C., and R. Zhang (2013), Multiphase chemistry of atmospheric amines, *Physical Chemistry*
495 *Chemical Physics*, *15*(16), 5738-5752, doi:10.1039/C3CP43446J.

496 Schwab, J. J., Y. Li, M. S. Bae, K. L. Demerjian, J. Hou, X. Zhou, B. Jensen, and S. C. Pryor
497 (2007), A laboratory intercomparison of real-time gaseous ammonia measurement methods,
498 *Environ Sci Technol*, *41*(24), 8412-8419, doi:10.1021/es070354r.

499 Silva, P. J., M. E. Erupe, D. Price, J. Elias, Q. G. J. Malloy, Q. Li, B. Warren, and D. R. Cocker,
500 III (2008), Trimethylamine as Precursor to Secondary Organic Aerosol Formation via Nitrate
501 Radical Reaction in the Atmosphere, *Environmental Science & Technology*, *42*(13), 4689-4696,
502 doi:10.1021/es703016v.

503 Smith, J. N., K. C. Barsanti, H. R. Friedli, M. Ehn, M. Kulmala, D. R. Collins, J. H. Scheckman,
504 B. J. Williams, and P. H. McMurry (2010), Observations of aminium salts in atmospheric
505 nanoparticles and possible climatic implications, *Proc. Natl. Acad. Sci.*, *107*(15), 6634-6639.

506 Wang, G., et al. (2016), Persistent sulfate formation from London Fog to Chinese haze,
507 *Proceedings of the National Academy of Sciences*, *113*(48), 13630-13635,
508 doi:10.1073/pnas.1616540113.

509 Wang, M., et al. (2020a), Rapid growth of new atmospheric particles by nitric acid and ammonia
510 condensation, *Nature*, *581*(7807), 184-189, doi:10.1038/s41586-020-2270-4.

511 Wang, Y., G. Yang, Y. Lu, Y. Liu, J. Chen, and L. Wang (2020b), Detection of gaseous
512 dimethylamine using vocus proton-transfer-reaction time-of-flight mass spectrometry,
513 *Atmospheric Environment*, *243*, 117875, doi:<https://doi.org/10.1016/j.atmosenv.2020.117875>.

514 Xiao, M., et al. (2021), The driving factors of new particle formation and growth in the polluted
515 boundary layer, *Atmos. Chem. Phys.*, *21*(18), 14275-14291, doi:10.5194/acp-21-14275-2021.

516 Xiao, S., et al. (2015), Strong atmospheric new particle formation in winter in urban Shanghai,
517 China, *Atmos. Chem. Phys.*, *15*(4), 1769-1781, doi:10.5194/acp-15-1769-2015.
518 Yan, C., et al. (2021), The Synergistic Role of Sulfuric Acid, Bases, and Oxidized Organics
519 Governing New-Particle Formation in Beijing, *Geophysical Research Letters*, *48*(7),
520 e2020GL091944, doi:<https://doi.org/10.1029/2020GL091944>.
521 Yao, L., et al. (2016), Detection of atmospheric gaseous amines and amides by a high-resolution
522 time-of-flight chemical ionization mass spectrometer with protonated ethanol reagent ions,
523 *Atmos. Chem. Phys.*, *16*(22), 14527-14543, doi:10.5194/acp-16-14527-2016.
524 You, Y., et al. (2014), Atmospheric amines and ammonia measured with a Chemical Ionization
525 Mass Spectrometer (CIMS), *Atmos. Chem. Phys.*, *14*, 12181-12194, doi:Doi: 10.5194/acpd-14-
526 16411-2014.
527 Yu, H., and S. H. Lee (2012), A chemical ionization mass spectrometer for the detection of
528 atmospheric amines, *Environ. Chem.*, *9*, 190-201.
529 Yu, H., R. McGraw, and S. H. Lee (2012), Effects of amines on formation of sub-3 nm particles
530 and their subsequent growth, *Geophys. Res. Lett.*, *39*, Doi: 10.1029/2011gl050099,
531 doi:10.1029/2011gl050099.
532 Zheng, J., Y. Ma, M. Chen, Q. Zhang, L. Wang, A. F. Khalizov, L. Yao, Z. Wang, X. Wang, and
533 L. Chen (2015), Measurement of atmospheric amines and ammonia using the high resolution
534 time-of-flight chemical ionization mass spectrometry, *Atmospheric Environment*, *102*, 249-259,
535 doi:<https://doi.org/10.1016/j.atmosenv.2014.12.002>.
536 Zhu, S., et al. (2022), Observation and Source Apportionment of Atmospheric Alkaline Gases in
537 Urban Beijing, *Environmental Science & Technology*, *56*(24), 17545-17555,
538 doi:10.1021/acs.est.2c03584.
539

1
2
3
4
5
6
7
8
9
10
11

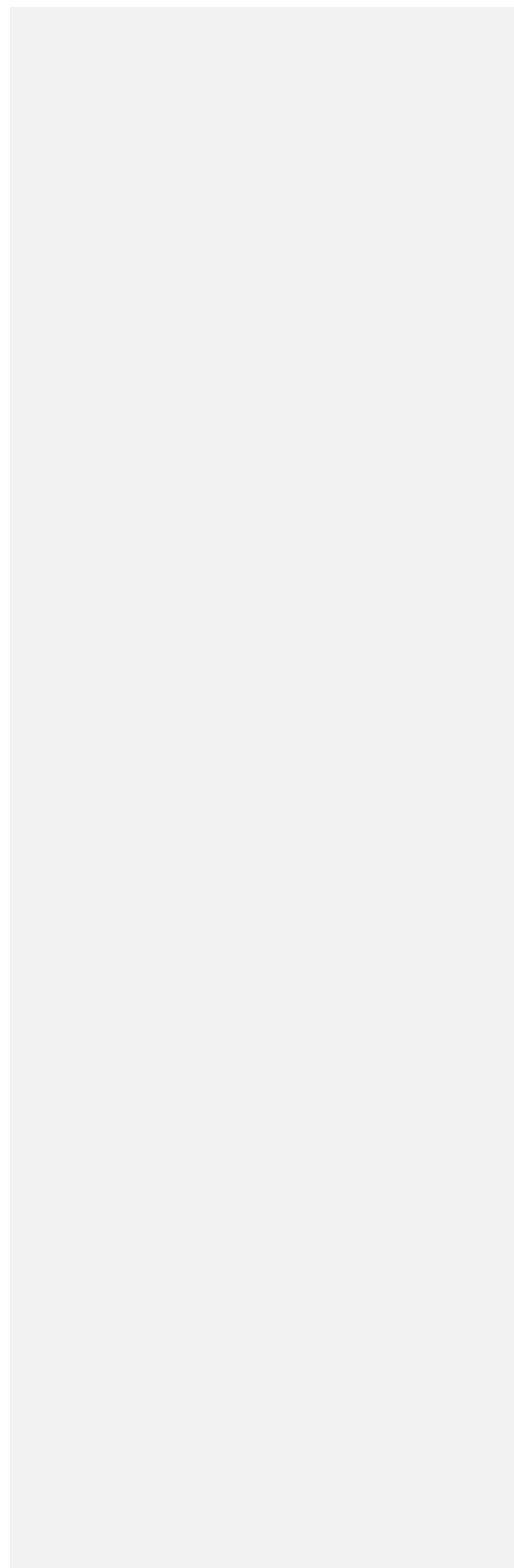
Supporting Information
Measurement Report: Urban Ammonia and Amines in Houston, Texas

Lee Tiszenkel¹, James Flynn², Shan-Hu Lee^{1*}

¹ Department of Atmospheric and Earth Sciences, University of Alabama at Huntsville;
Huntsville, Alabama, USA

² Department of Earth and Atmospheric Sciences, University of Houston; Houston, Texas, USA

Corresponding author (shanhu.lee@uah.edu)



12 **Table S1111**, CIMS sensitivities and detection limits for ammonia and amine measurements
 13 during this study in Houston. The sensitivities (Hz pptv⁻¹) shown here are normalized for
 14 1,000,000 Hz reagent ion signals. The detection limits are estimated as three times the standard
 15 deviation of the background signal over one minute of background measurements. In
 16 comparison, we also included those previously reported with the same instrument nearly 10 years
 17 earlier by [You *et al.*, 2014], estimated with the same time resolution.

Deleted: 1

Deleted: are estimated using a 1-min integration time

Deleted: .

Compound	Sensitivity (Hz pptv ⁻¹ MHz ⁻¹)	Detection limit (pptv)	Sensitivity[You <i>et al.</i> , 2014] (Hz pptv ⁻¹ MHz ⁻¹)	Detection limit[You <i>et al.</i> , 2014] (pptv)
Ammonia	13.1 ± 0.87	128.4	13	35
C1 amine	8.6 ± 0.06	0.4	12	0.1
C2 amine	2.6 ± 0.02	0.7	12	0.5
C3 amine	4.3 ± 0.03	1.2	8	0.8
C4 amine	2.3 ± 0.02	3.6	4	3.3
C5 amine	1.3 ± 0.01	2.7	2	1.9
C6 amine	1.3 ± 0.01	2.6	2	1.4

19
20

24 **Table S2.** Relationships of the measured concentrations of each amine ammonia derived from the
25 combined observations in Houston reported by this study and Kent, Ohio reported by [*You et al.*,
26 2014].

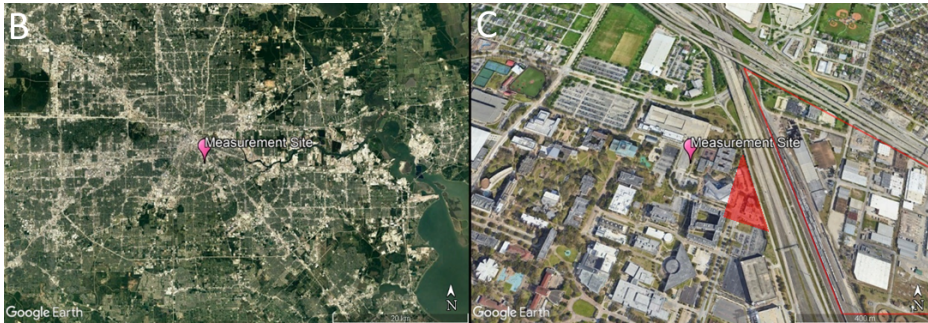
27

Amine	Relationship to ammonia in pptv
C1	1.1×10^{-3} [NH ₃]
C2	1.4×10^{-3} [NH ₃]
C3	8.4×10^{-3} [NH ₃]
C4	No correlation
C5	1.9×10^{-2} [NH ₃]
C6	3.5×10^{-3} [NH ₃]

28

29

30

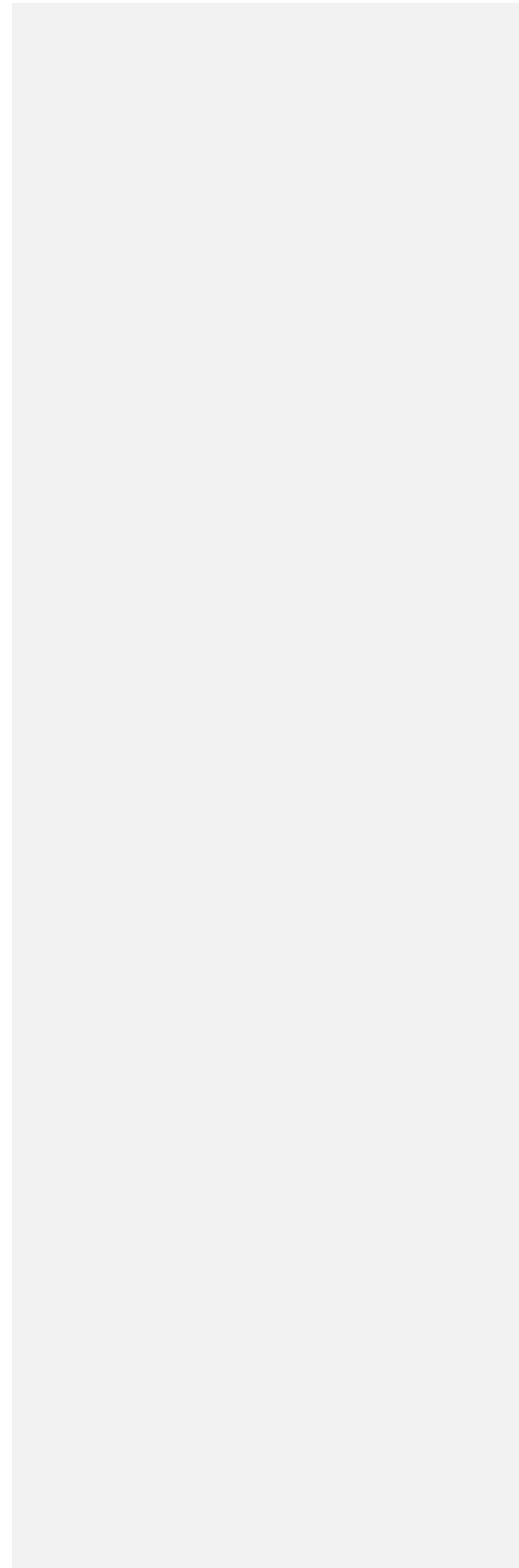


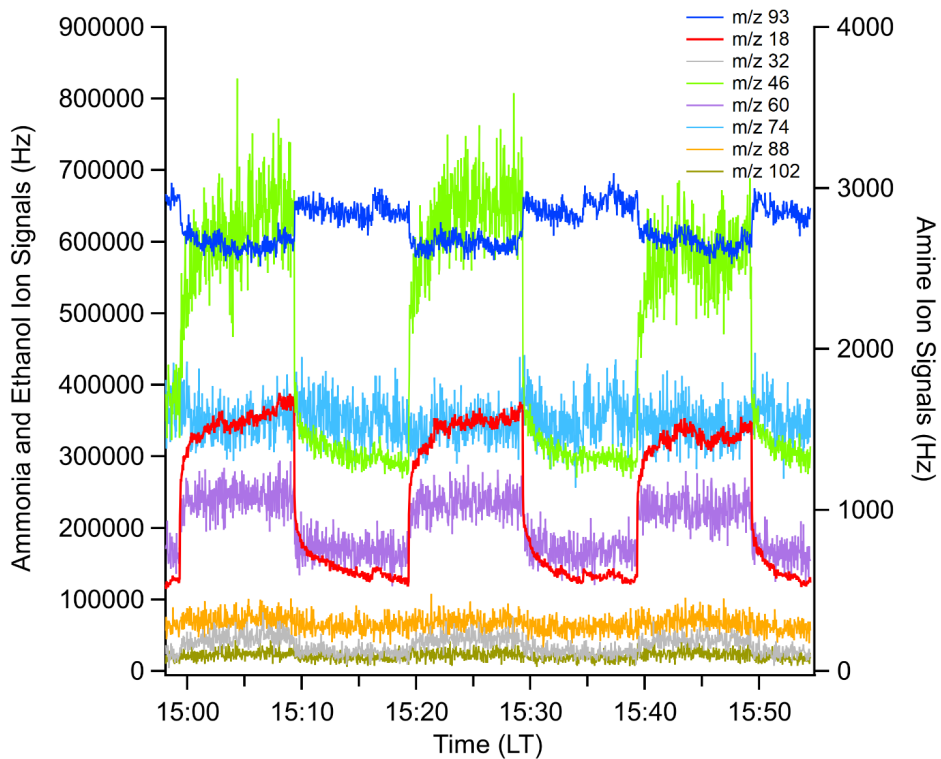
31

32

33 **Figure S1.** (a) Measurement site in the greater Houston urban area. The site was SE of the city
34 center and located NW of Tranquility Bay. (b) Satellite view of the nearby vicinity of the
35 measurement site. The University of Houston campus is seen in the lower left. The highways, a
36 train yard, and industrial areas are seen in the lower right. The upper right shows the nearby
37 residential zone.

38

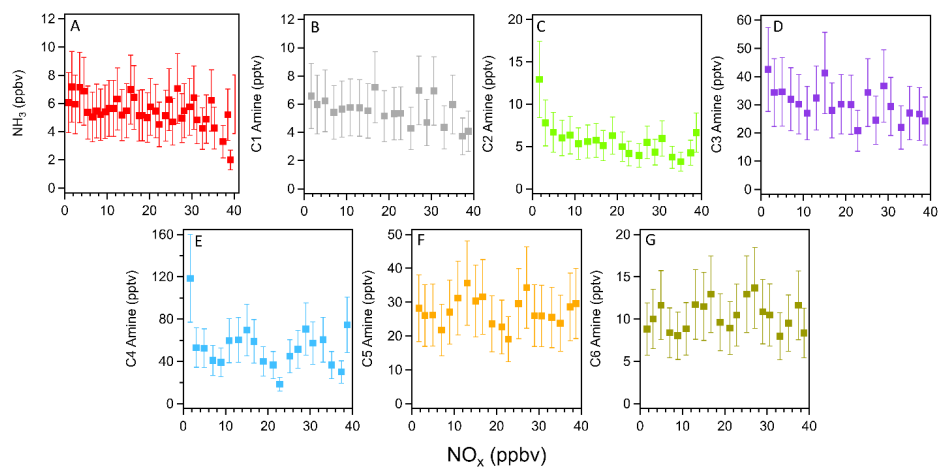




39
 40
 41
 42
 43
 44
 45
 46

Figure S2. A time series of the measurement/background cycle of the CIMS. This shows three switches of the inlet flow between ambient measurement and the phosphate scrubber. At 15:49, the flow was switched to background mode and the response of the NH_4^+ signal (m/z 18) immediately dropped. The NH_4^+ signal continues to decrease after the drop, and the signal reaches an e-folded concentration within 28 seconds.

47

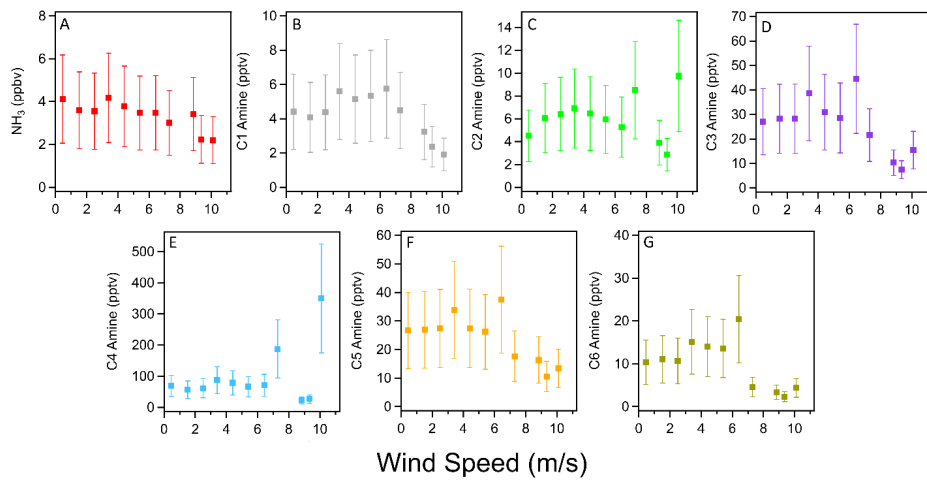


48

49

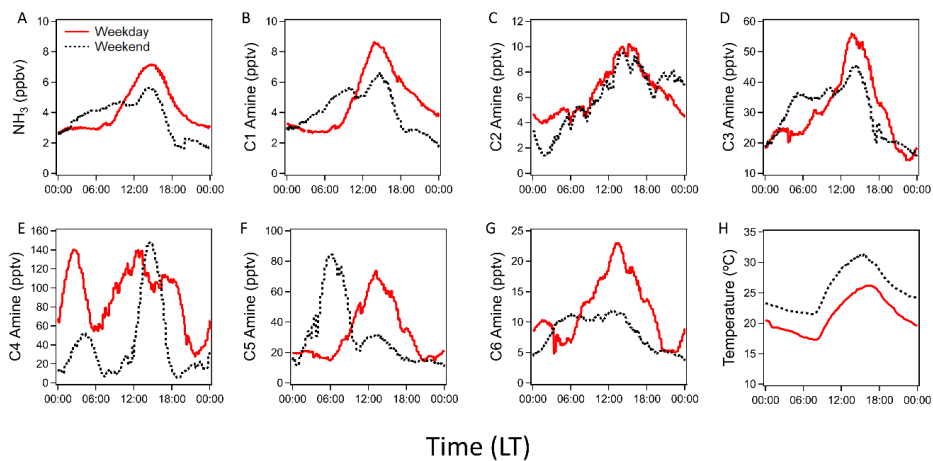
50 **Figure S3.** Correlation between (a) ammonia and (b-g) C1-C6 amines with the collocated NO_x
51 concentrations during the measurement campaign. Vertical bars indicate one standard deviation
52 from the mean values of observation data.

53



54
55
56
57
58

Figure S4. Correlation of (a) ammonia and (b) C1-C6 amines with wind speed throughout the observation period.



59
 60 **Figure S5.** Diurnal cycles of (a) ammonia, (b-g) amines, and (h) temperature on weekdays (solid
 61 red) vs weekends (dashed black).
 62

63

64 **References**

65 You, Y., et al. (2014), Atmospheric amines and ammonia measured with a Chemical Ionization
66 Mass Spectrometer (CIMS), *Atmos. Chem. Phys.*, *14*, 12181-12194, doi:Doi: 10.5194/acpd-14-
67 16411-2014.

68

